沸水式反應器壓力邊界異材銲道腐蝕疲勞行為研究

黃俊源、 楊明宗 、鄭勝隆
劉如峰 、郭榮卿

2009中華核能學會年會暨用過核燃料管理策略研討會

核 能 研 究 所

98年12月16日

Outlines

1. Introduction
2. Objectives
3. Experimental procedures
4. Results and discussion
5. Conclusions

1. Introduction

1) Incidences of stress corrosion cracking of Alloy 182 weld in both BWRs and PWRs have been reported.

2) Alloy 52, which has a higher chromium content than Alloy 182/82, has been used to repair the defected CRDM/thermocouple penetration nozzles, pressurizer nozzles and hot leg nozzles, etc. because of its superior SCC resistance.

1. Introduction

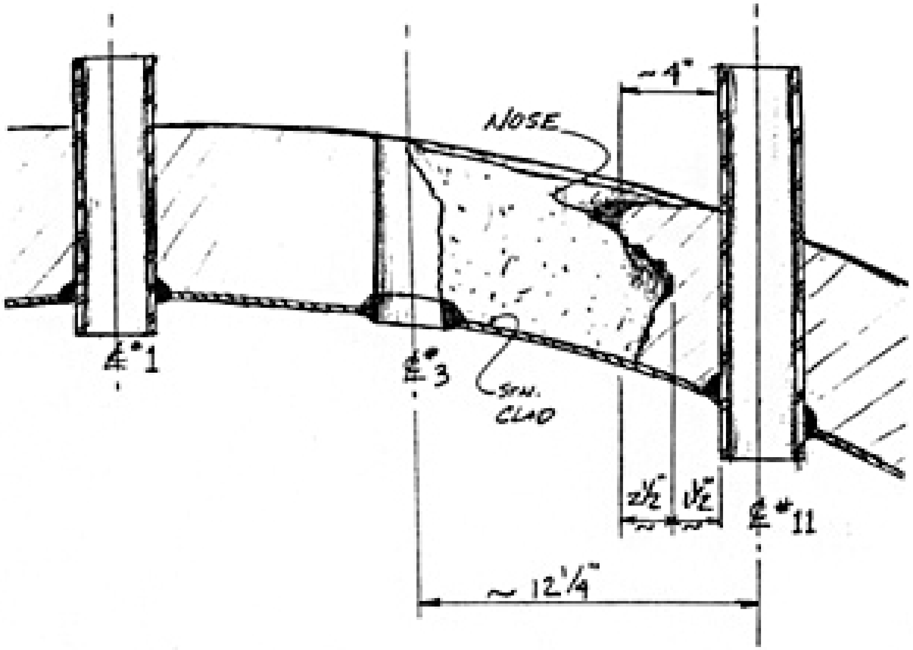

Davis-Besse Reactor with a Hole in its Head

Example of Cracking in R/V Head Penetration Nozzle

Bugey-3（France）（’91）

Axial cracking in base metal

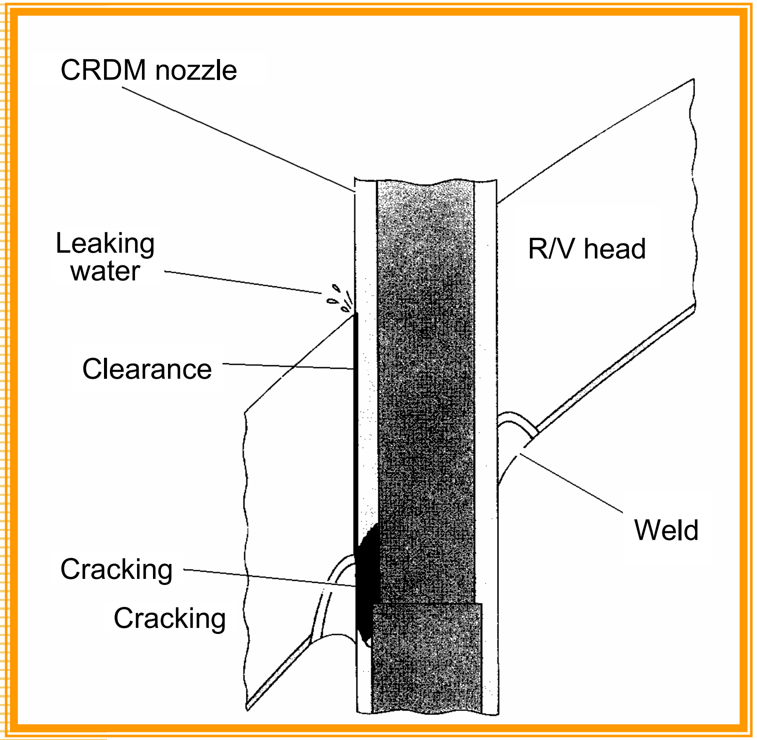

Oconee-3（U.S.)（’01）start of operation：December 1974

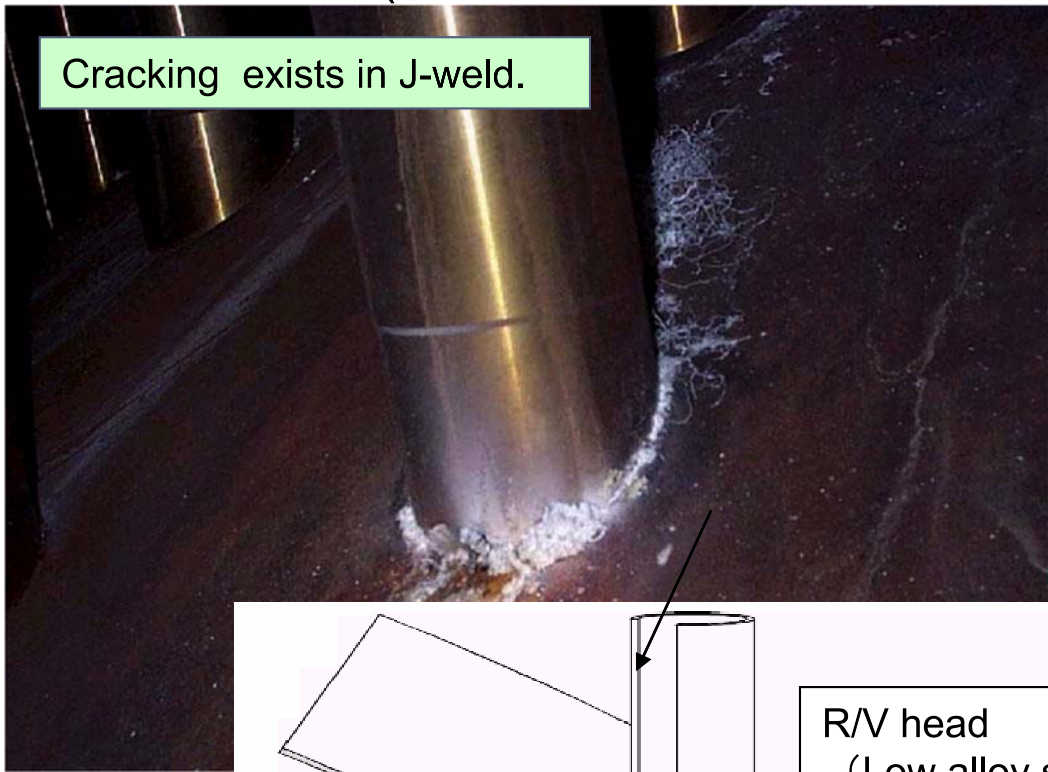

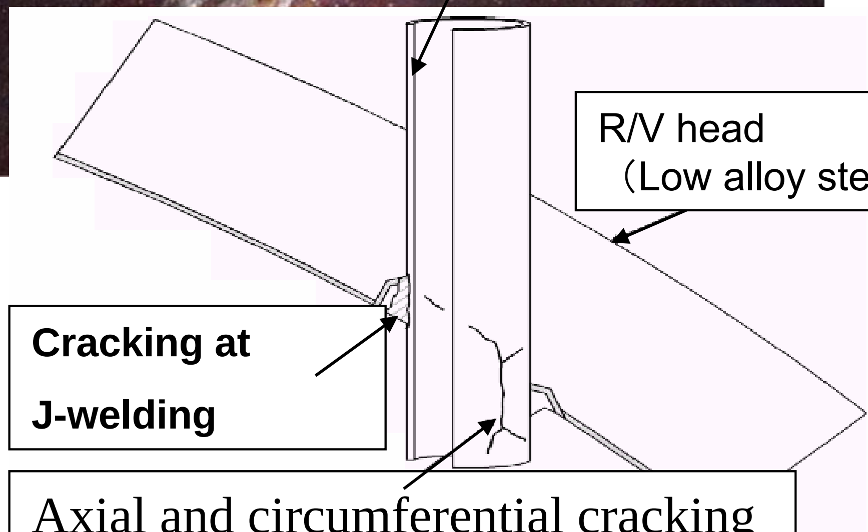

Example of Cracking in Pressurizer nozzle

Tsuruga 2 Pressurizer Relief Nozzle Safe-end Leakage

Top of Pressurizer

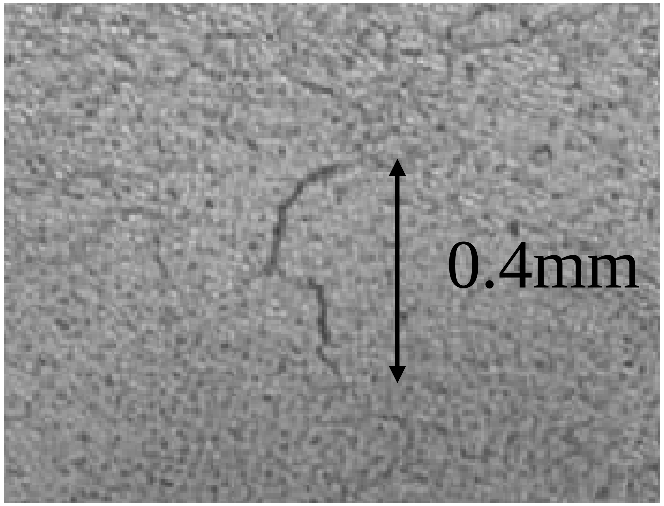

Micro Printing Result

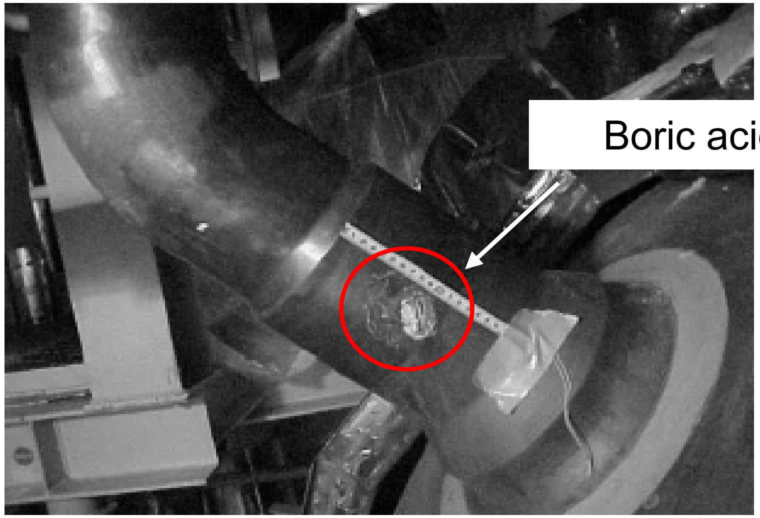

Safe-end Weld

Reference: Nuclear and Industrial Safety Agency, Ministry of Economy, Trade and Industry

1. Introduction

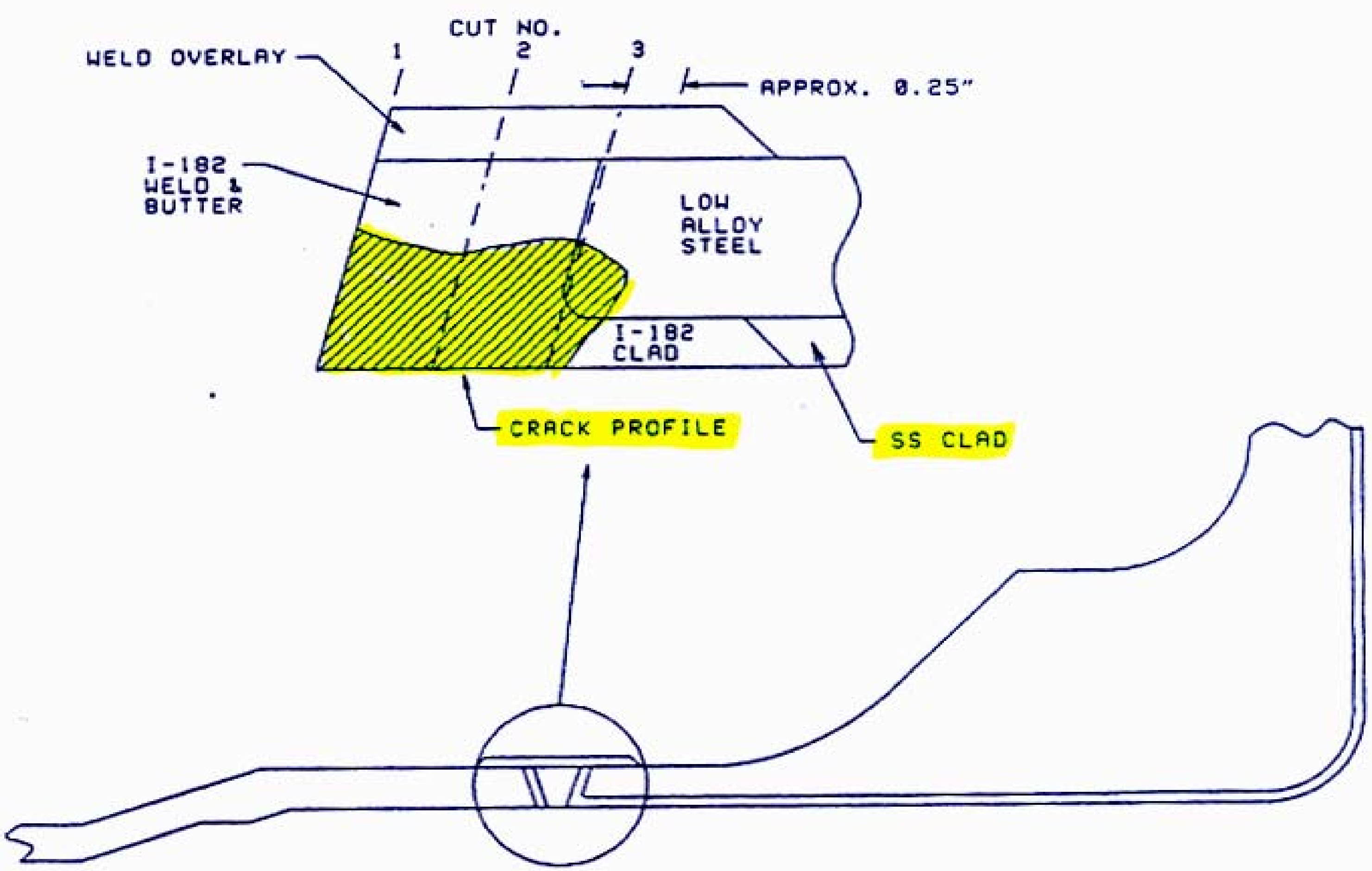

Fig. 3. Crack profile – Chinshan 2 N2E nozzle (recirculation inlet).

計畫背景

BWR

A182/A82銲道破損案例

Date	Plant	Component
1978	Duane Arnold	Recirculation inlet nozzle
Spring 1986	Vermont Yankee	Core spray nozzle
1986 & 1987	Chinshan units 1 and 2	Recirculation inlet nozzle
Fall 1988	Brunswick units 1 and 2	Recirculation inlet nozzle Core spray nozzle
Spring 1991	River Bend	Feedwater nozzle
Spring 1996	Brunswick units 1 and 2	Feedwater nozzle
Fall 1997	Hope Creek	Core spray nozzle
Spring 1998	Nine mile point unit 2	Feedwater nozzle
Spring 1999	Perry	Feedwater nozzle
Fall 1999	Duane Arnold	Recirculation inlet nozzle
2001	Hamaoka	CRD Housing
2001	Tsuruga	Core shroud support structure
2005	Chinshan unit 1	Recirculation outlet nozzle
2005	Kousheng unit 2	Recirculation outlet nozzle

計畫背景

PWR

A182/A82銲道破損案例

Date	Plant	Component
1991	Bugey unit 3	CRDM nozzle
2000	Ringhals units 3 and 4	Hot leg nozzle
2000	VC Summer	Hot leg nozzle
2001	Oconee-1	CRDM nozzle and thermal couple nozzle
2001	Oconee-3	CRDM nozzle
2001	Arkansas	CRDM nozzle
2002	Davis-Besse	CRDM nozzle
2003	Tsuruga	PZR relief and safety nozzle
2005	Cook 1	PZR safety nozzle
2006	Millstone 3	PZR spray nozzle
2006	SONGs 2	PZR safety nozzle PZR spare nozzle
2006	Davis Besse	Cold leg drain
2006	Calvert Cliffs 1	PZR relief nozzle
2006	Calvert Cliffs 1	Hot leg drain
2006	Wolf Creek	PZR relief, safety and surge
2007	Farley 2	PZR

1. Introduction

(3) The transitional region of the dissimilar metal weldment(DM) is noted to have a complex microstructure, welding residual stress and wide variations in chemical composition.

2. Objectives

1) To study the corrosion fatigue crack growth rate of the dissimilar metal weldment **under nominal constant ΔK**.

2) To investigate the effects of **the transitional region** of the DM on the corrosion fatigue crack growth rate.

3. Experimental procedures

Alloy 52-A508 weldment

Nominal constant ΔK fatigue crack growth rate tests in BWR reactor coolant environments

Welding residual stress measured by numerical analysis and hole drilling method

SEM

Crack closure measured along the crack length

Degradation mechanism analysis

Chemical composition of A508 low alloy steel

Designation	Composition (wt%)									
	C	Si	Mn	P	S	Ni	Mo	V	Cr	Fe
A508F1	0.16	0.21	1.35	0.005	0.005	0.76	0.57	0.014	0.13	Bal.
A508F2	0.15	0.22	1.36	0.005	0.015	0.82	0.52	0.013	0.15	Bal.

Chemical Composition of Alloy 52

Composition (wt%)															
C	Mn	Fe	S	Si	Cu	Ni	Cr	Al	Ti	Co	Mo	P	Nb+Ta	Al+Ti	others
0.024	0.24	8.07	< 0.001	0.15	0.01	61.44	28.8	0.72	0.51	0.009	0.01	0.003	0.01	1.23	< 0.5

Test condition of high-temperature water environment

Test parameters	Values
Pressure, MPa	10
Temperature, ℃	300
Conductivity(inlet), μScm^{-1}	0.06
Conductivity(outlet), μScm^{-1}	0.08
Oxygen(inlet),	6.8 ppm
Oxygen(outlet),	7.8 ppm
ECP(SHE)	0.2 volt
pH(inlet)	6.5
pH(outlet)	6.6
Autoclave exchange rate	1 time/h

Sampling scheme for the dissimilar metal weldment

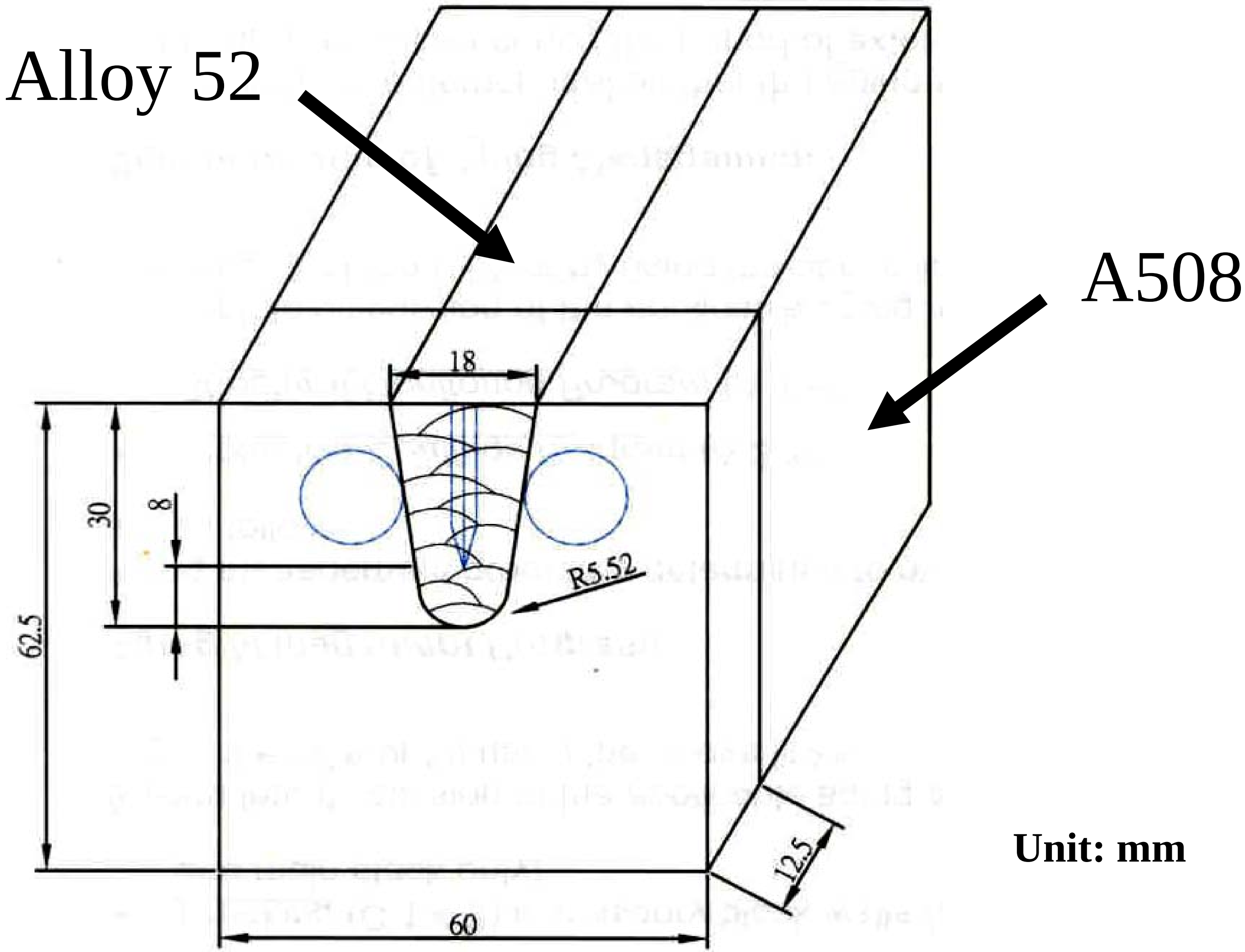

Unit: mm

4. Results and discussion

1) **Fatigue crack growth rate measurements for Alloy 52-A508 weldment at 300 ℃ in air**
2) **Nominal constant ΔK test in high temperature water environment**
3) **Welding residual stress analysis and measurement**
4) **Fatigue crack closure measurement**

1) Fatigue crack growth rate measurements for Alloy 52-A508 weldment

Fatigue crack growth rate against stress intensity factor range for Alloy 52-A508 weldment tested at 300℃ in air

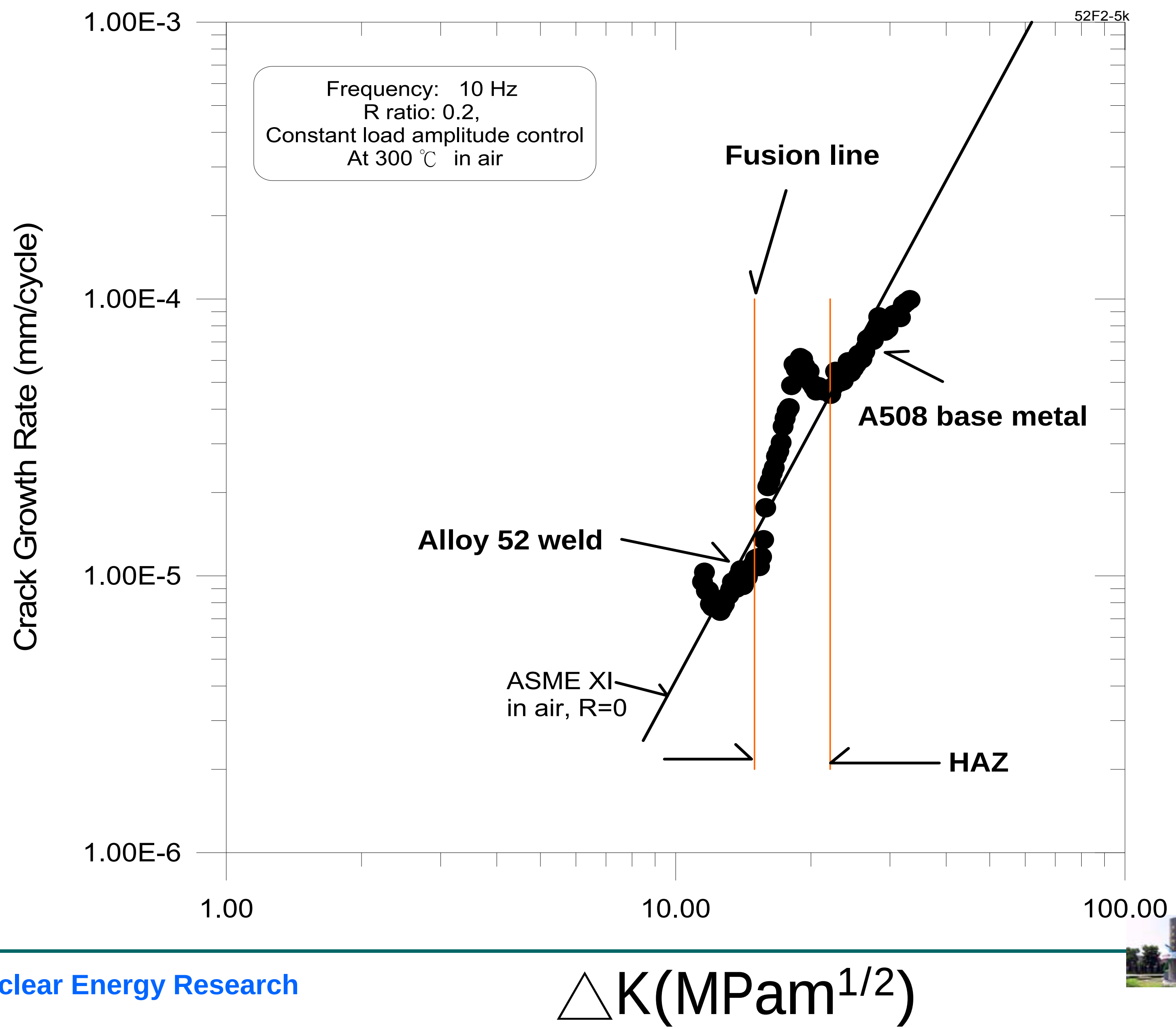

Fatigue crack growth rate overshoot in the HAZ. It could be related to the residual stress, higher hardness and complicated microstructure.

Fatigue fracture surface of Alloy 52-A508 weldment

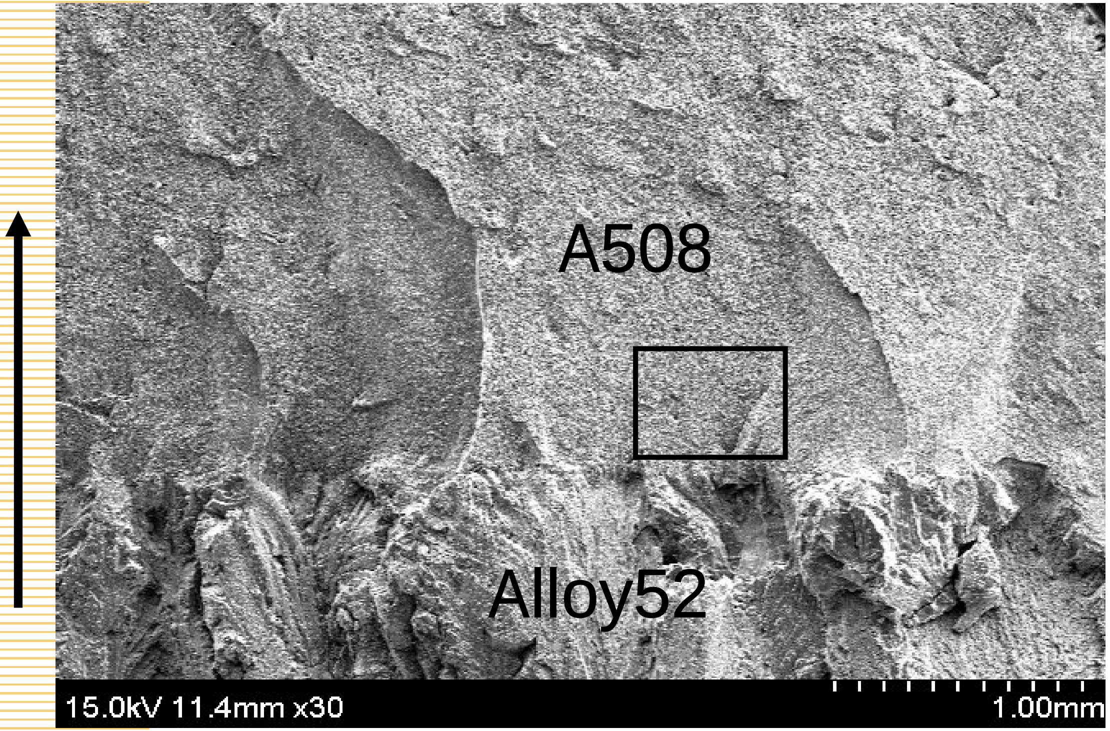

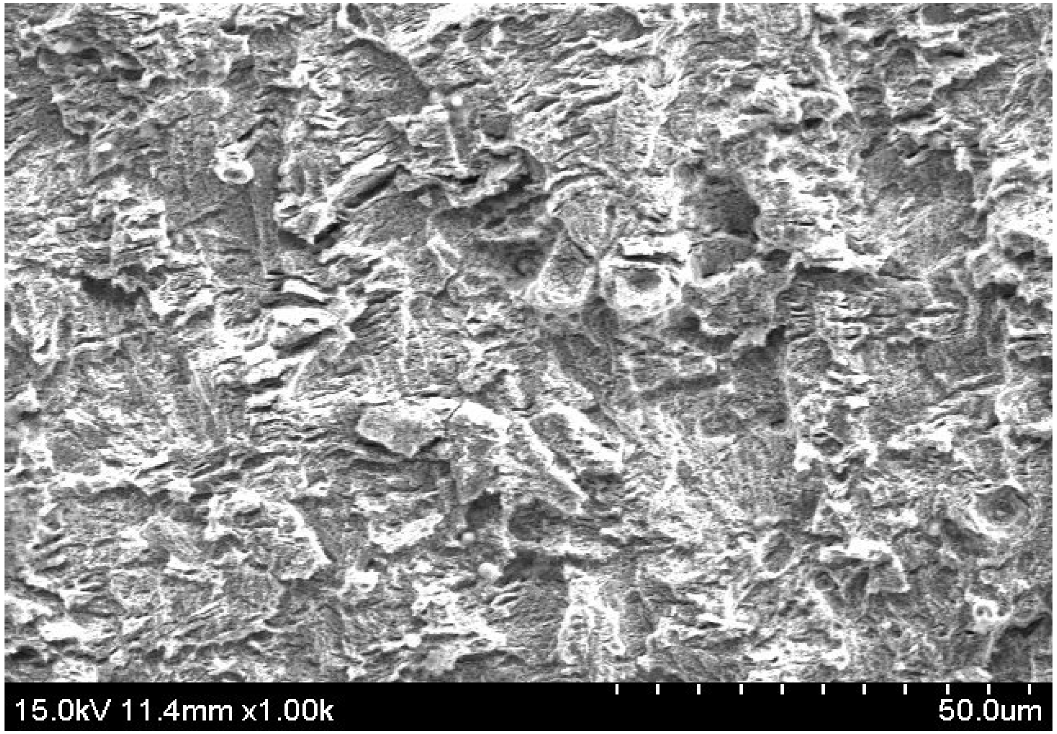

(a) macroscopic fracture surface showing the quasi-cleavage-like surface of the heat-affected zone

(b) showing brittle striations at a higher magnification.

(2) Nominal constant ΔK test in high temperature water environment

A schematic disposition of the ACPD probes

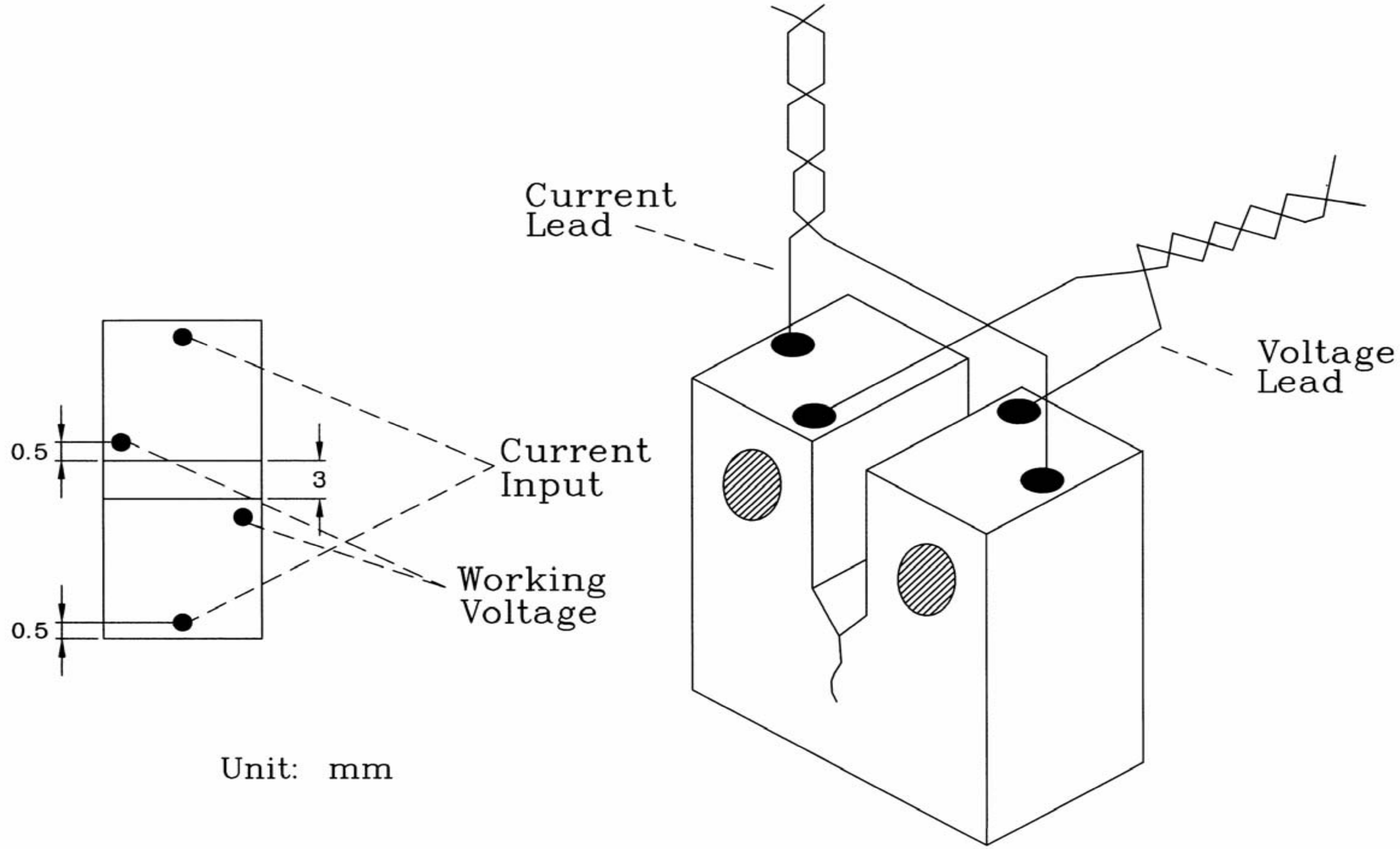

Fatigue crack growth behavior of Alloy 52-A508 specimen without a side groove on each side in the high temperature water environment.

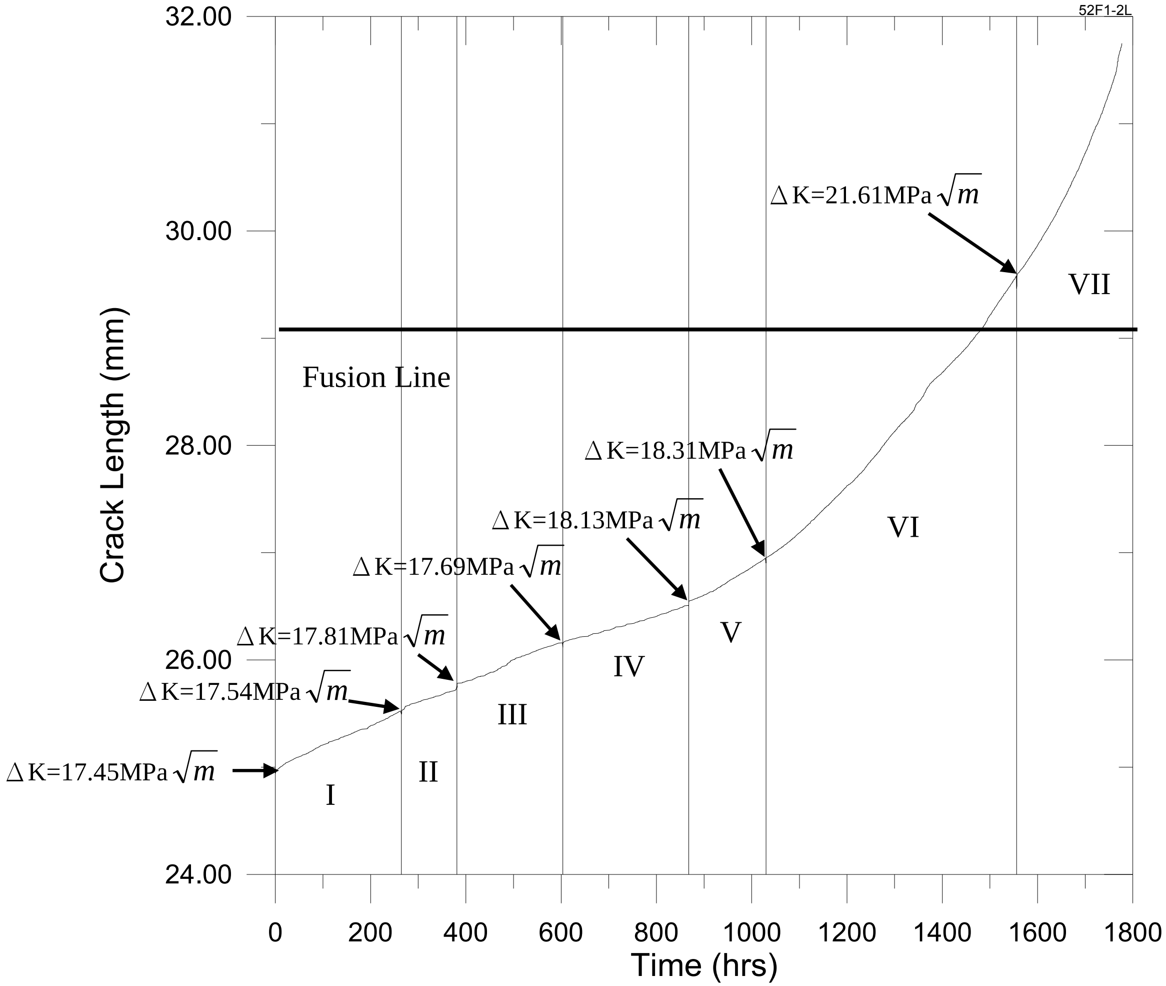

Unit: mm/sec

I	II	III	IV	V	VI	VII
5.79×10^{-7}	5.78×10^{-7}	4.72×10^{-7}	4.01×10^{-7}	6.95×10^{-7}	1.35×10^{-6}	2.87×10^{-6}

Fatigue crack growth behavior of Alloy 52-A508 specimen with a side groove on each side in the high temperature water environment.

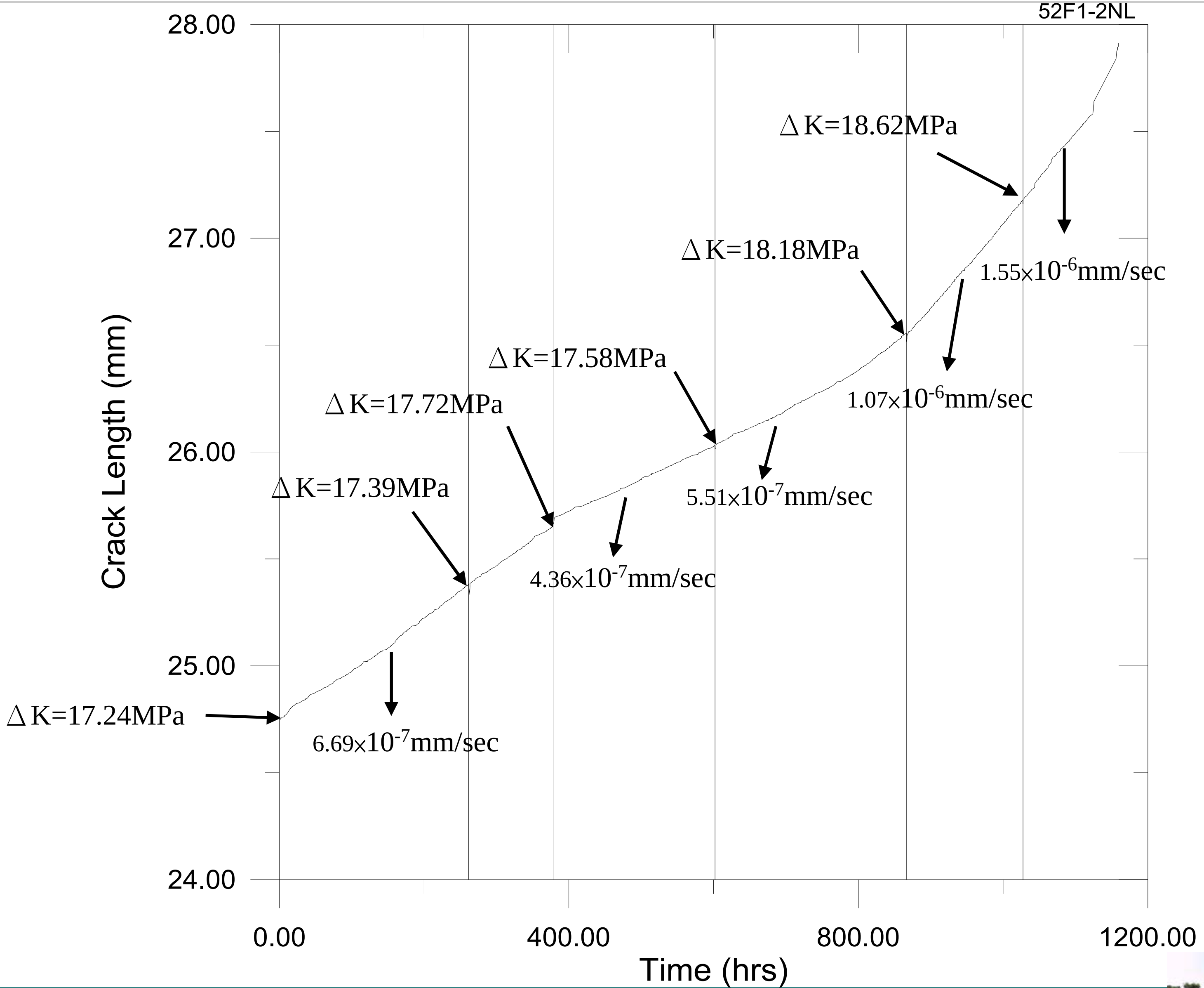

A comparison of fatigue crack growth behavior for Alloy 52-A508 weldment with and without groove in high temperature water environment.

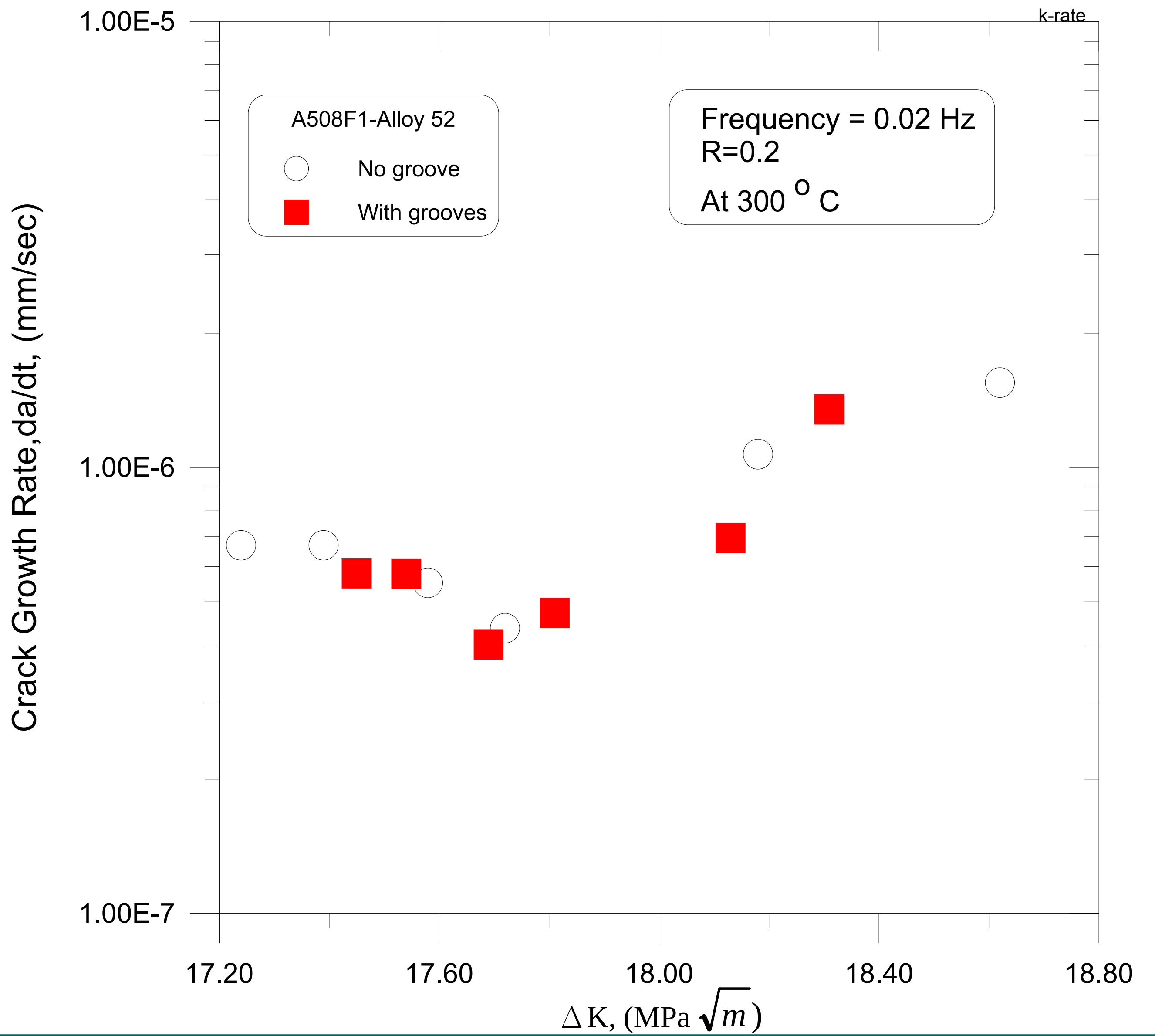

Alloy 52-A508F2異材銲道於300℃空氣中定應力強度因子之裂縫生長曲線圖

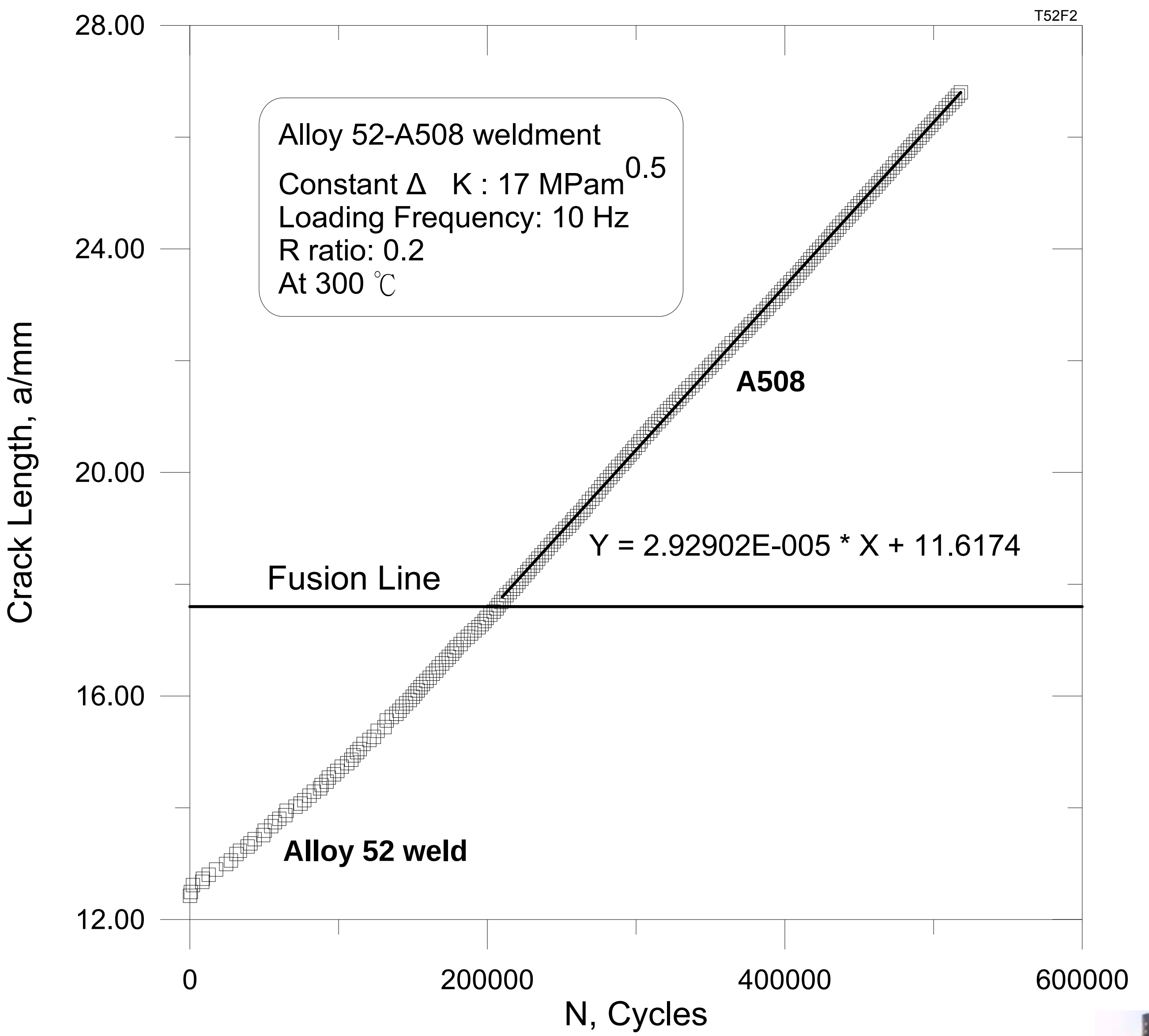

SS316L 於室溫空氣中定應力強度因子之裂縫生長曲線圖

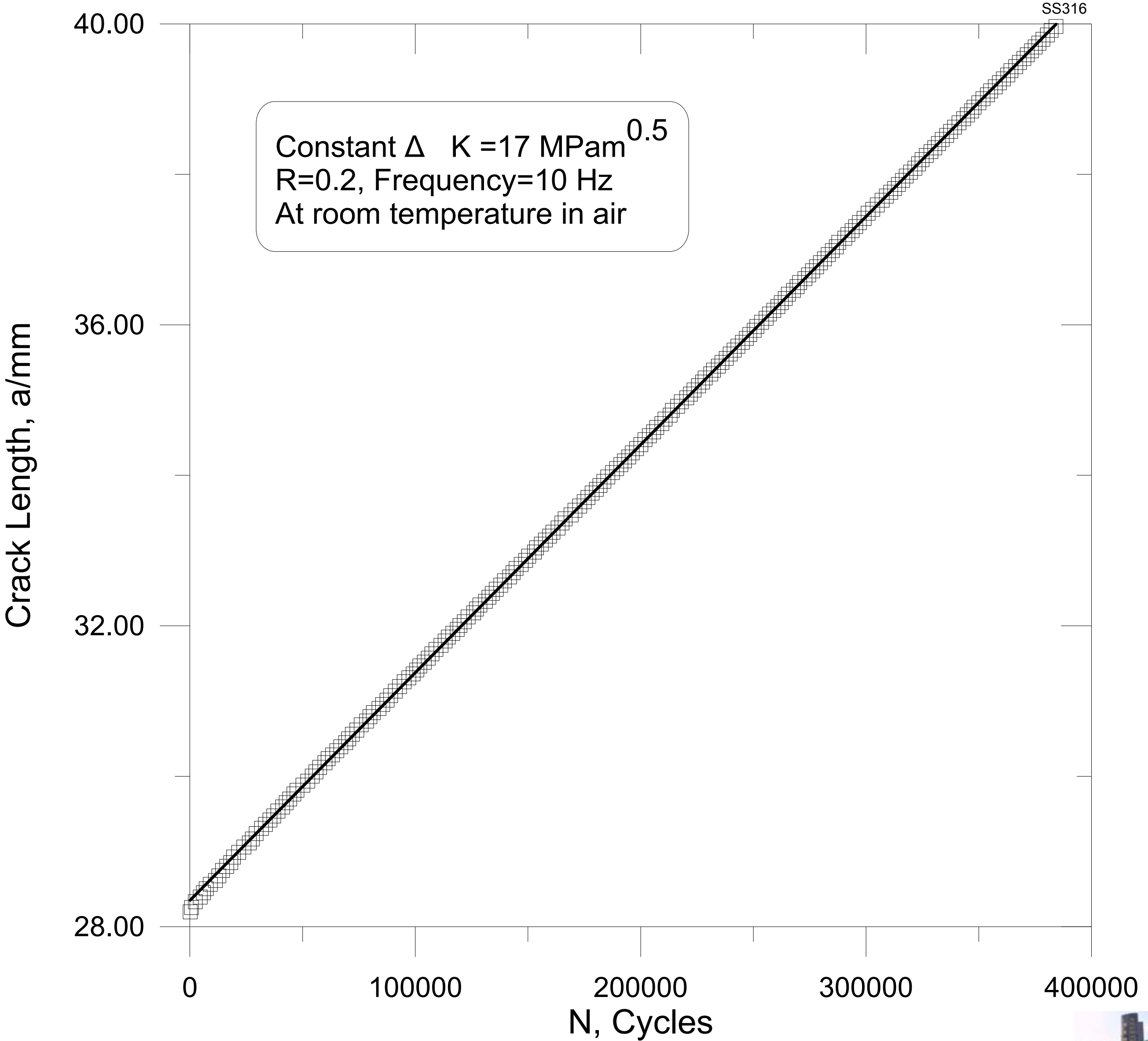

Corrosion fatigue crack growth rates increasing with the crack advance might be due to

1) An increase in the tensile residual stress and a decrease in crack closure effects in the Alloy 52 weld.

2) Macro-composition transition from the bottom to the center of the weld.

(3) Welding residual stress analysis and measurement

Residual stress measurement in front of the specimen notch

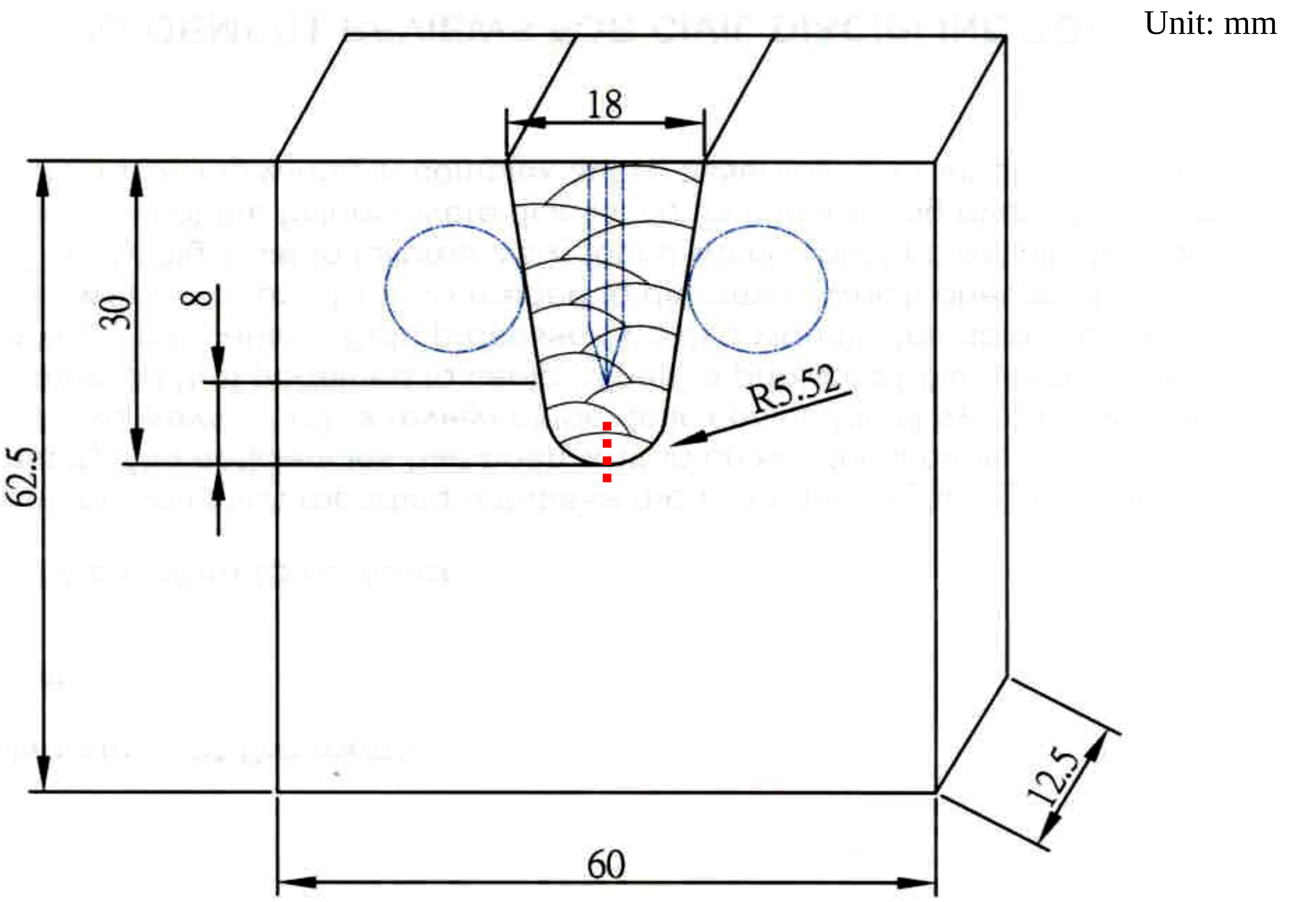

Residual stress measurement in front of the specimen notch

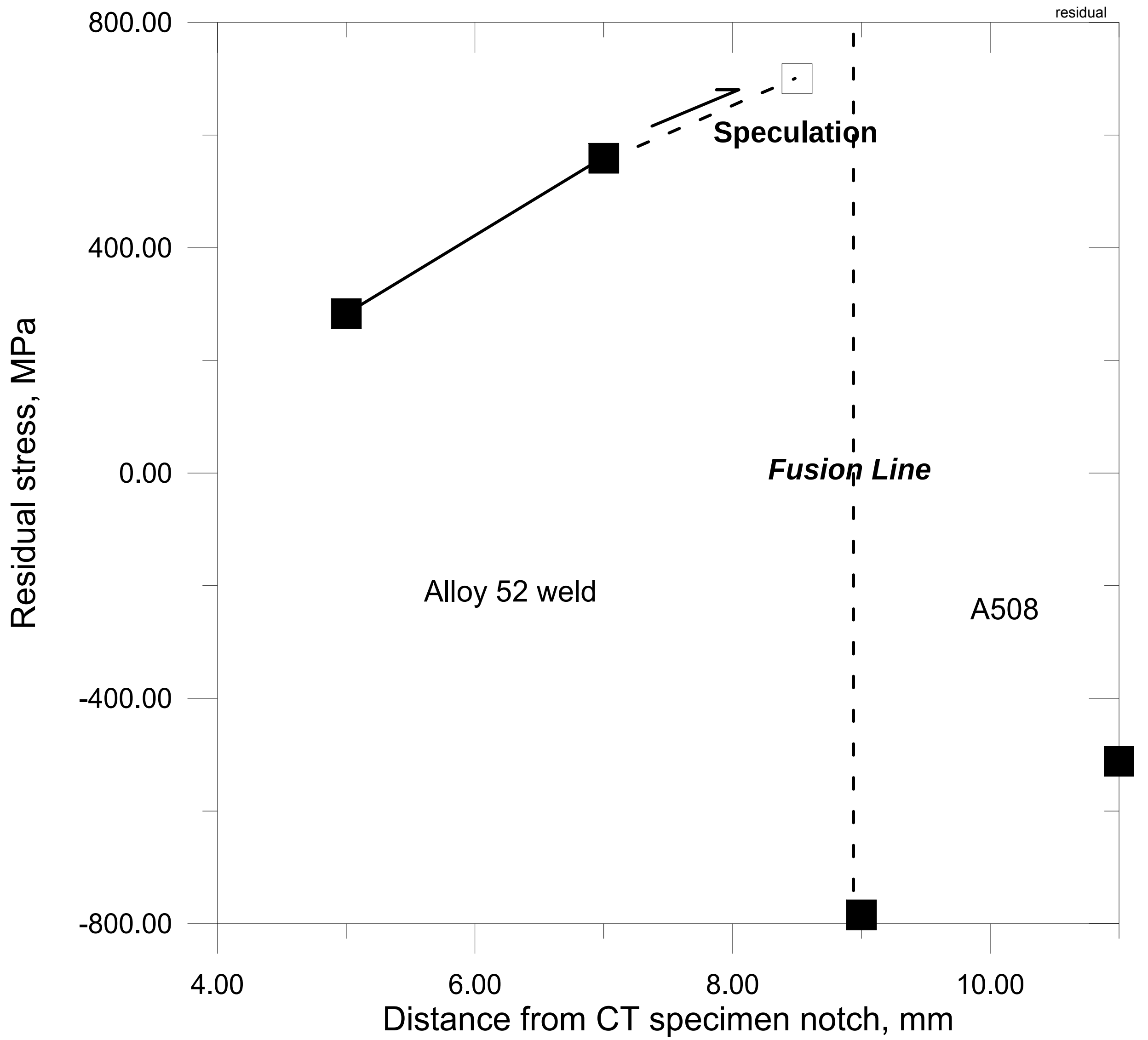

An increase in the residual tensile stress with the weld depth

FEM model for the Alloy 52-A508 weldment.

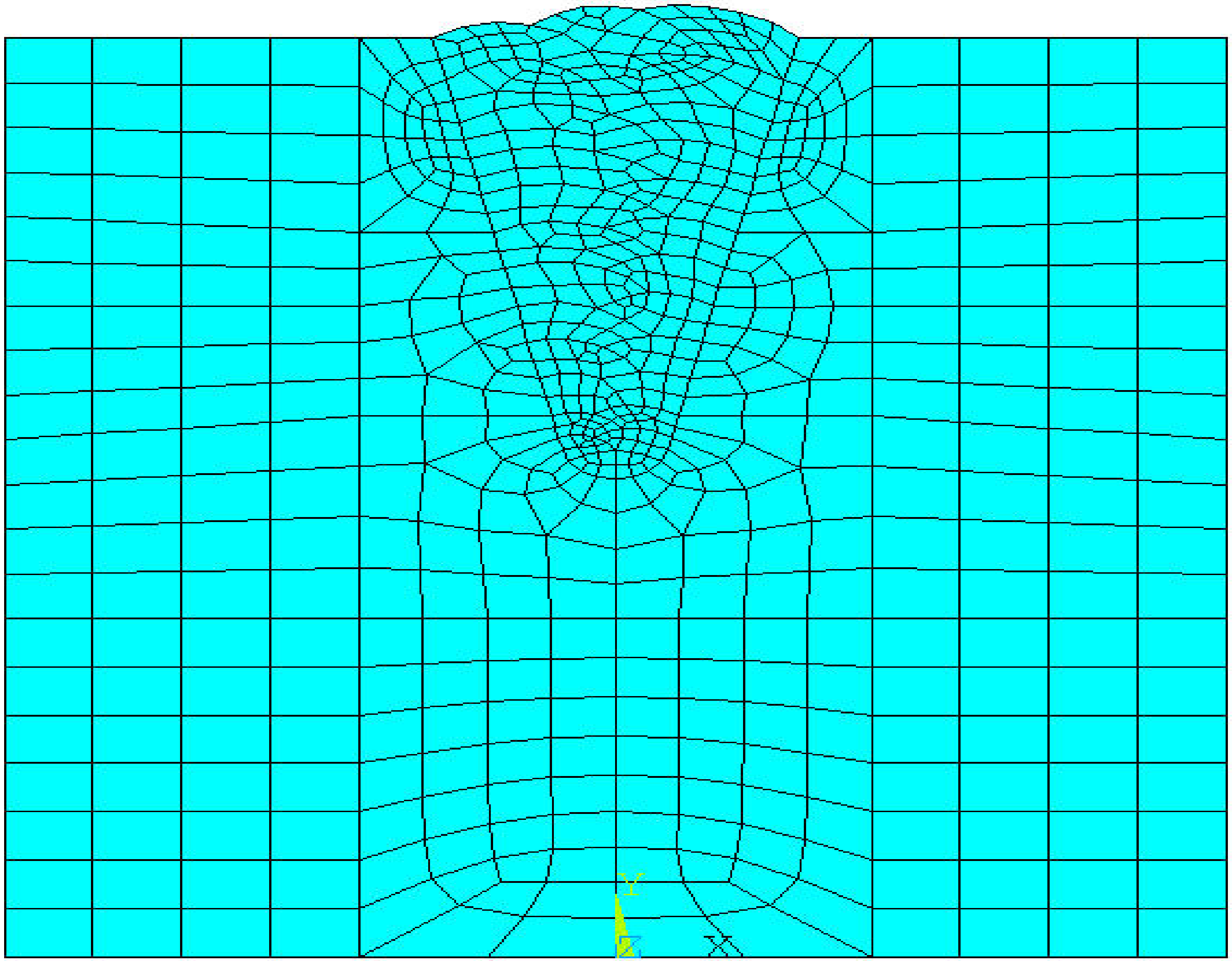

Welding residual stress distribution for Alloy 52-A508 weldment.

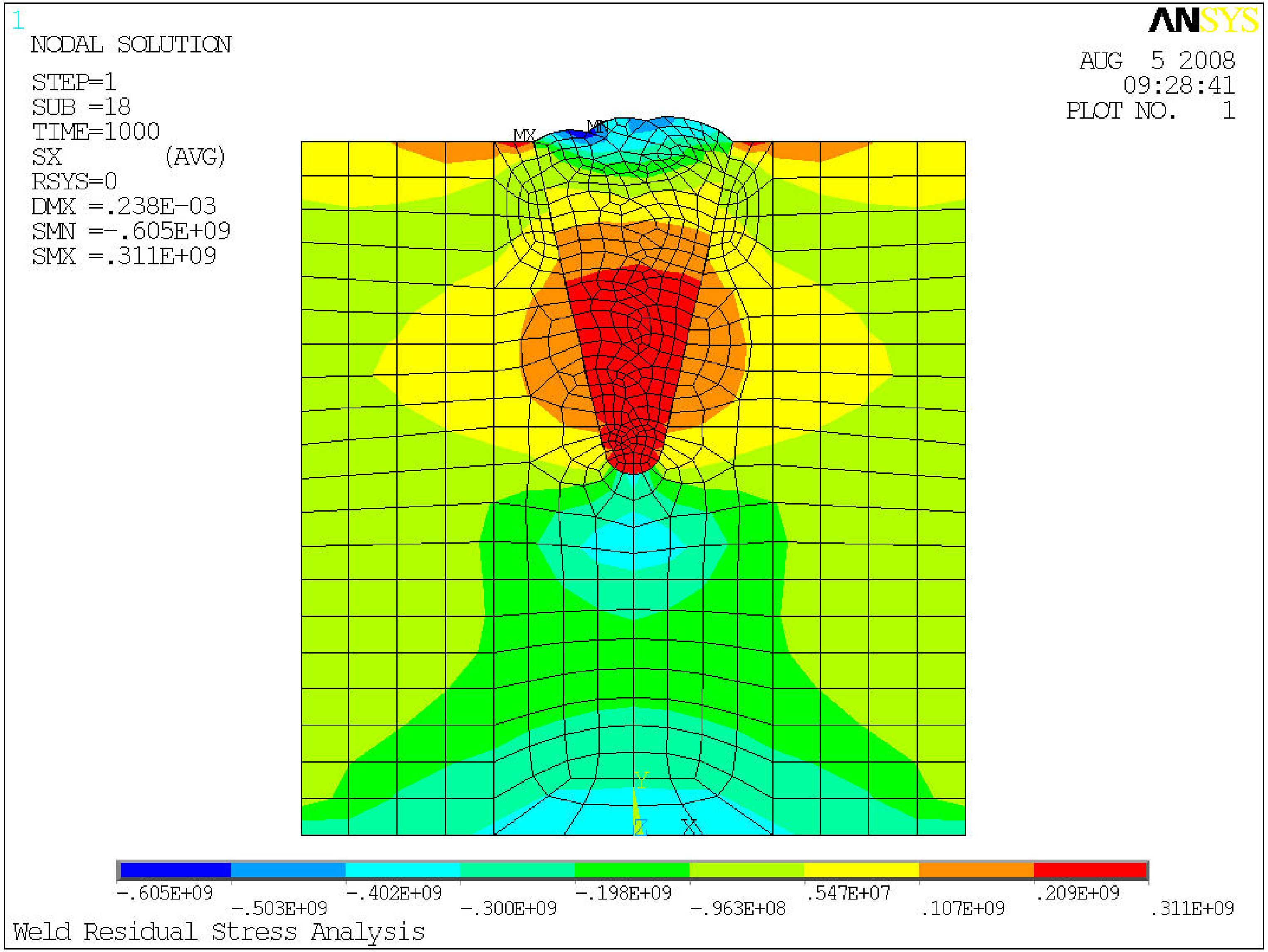

A comparison between analytic results and experimental measurements on the welding residual stress.

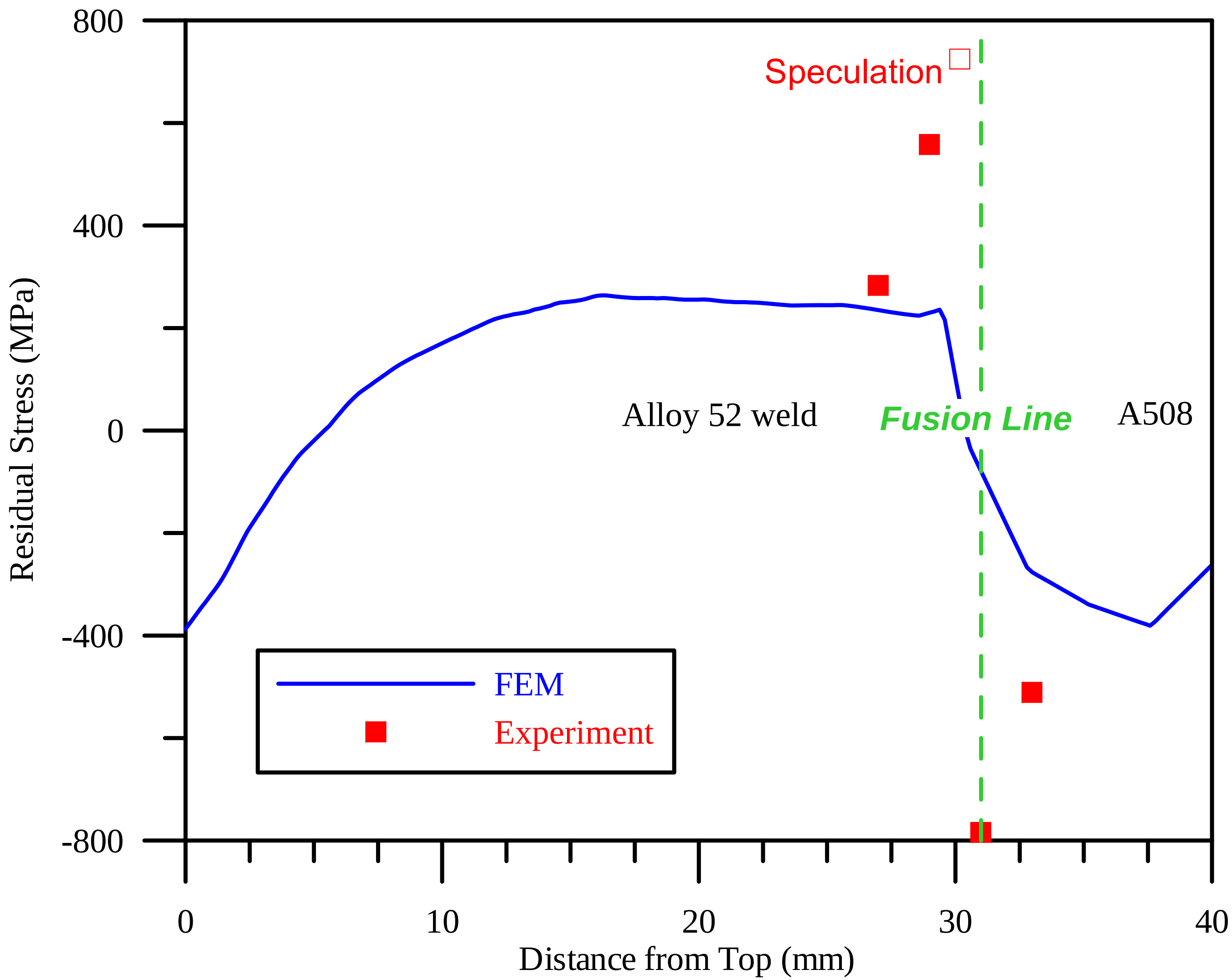

Fracture surface of Alloy 52-A508 weldment at a loading frequency of 0.02 Hz in a simulated BWR water environment.

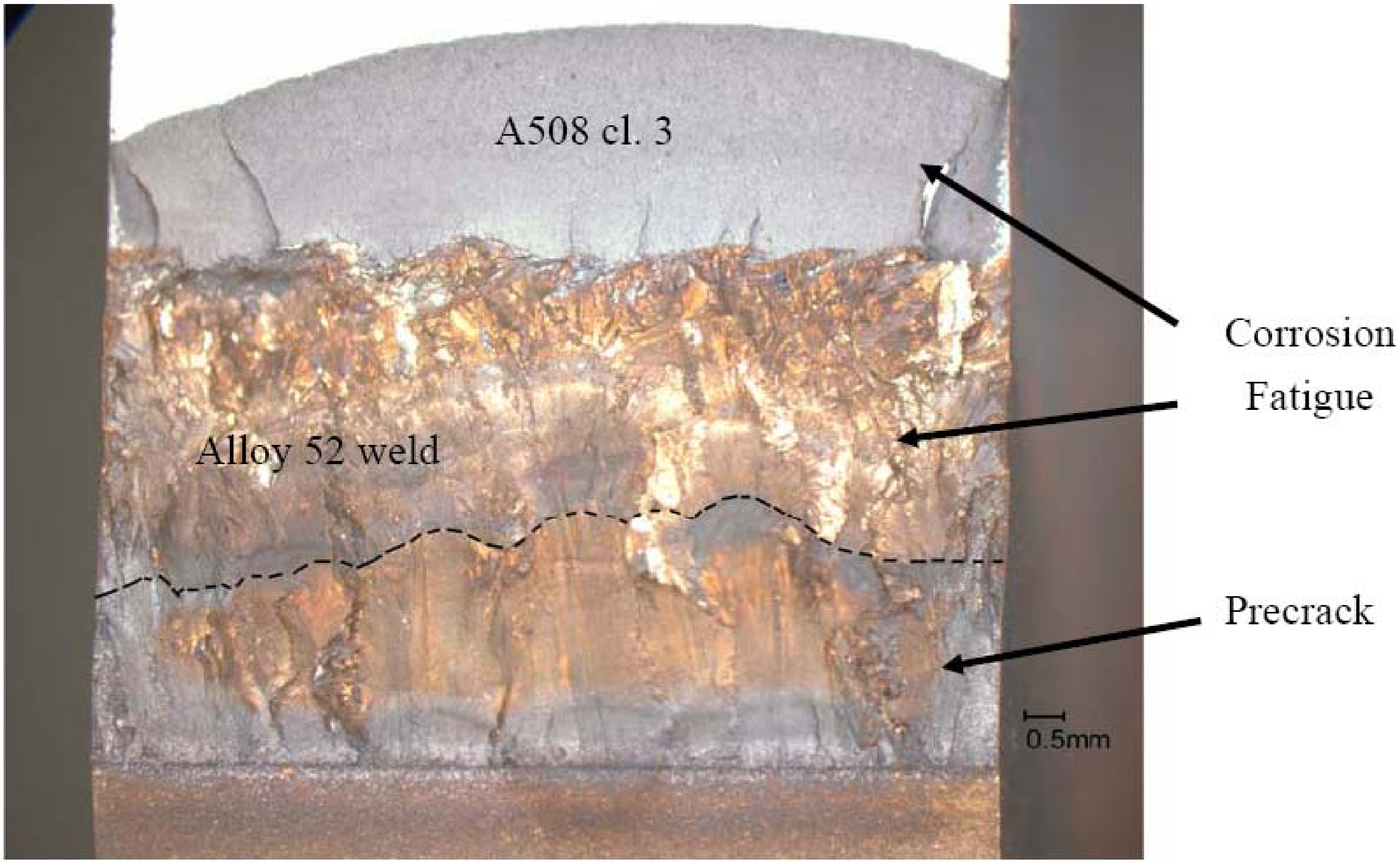

(4) Fatigue crack closure measurement

Fatigue crack closure measurement in front of the specimen notch

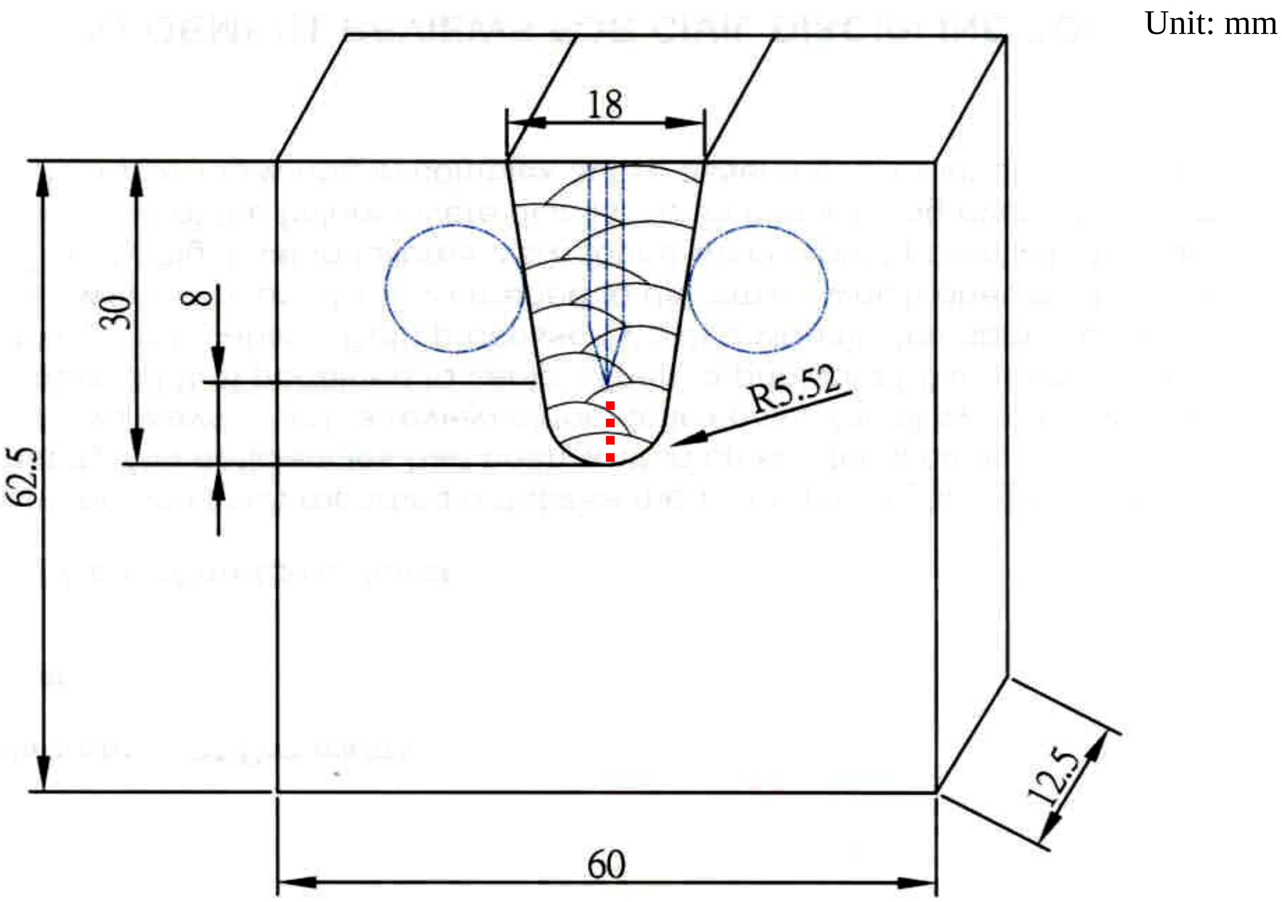

Crack opening stress intensity factor, Kop, was determined by the intersection of the two secants of uploading curve.

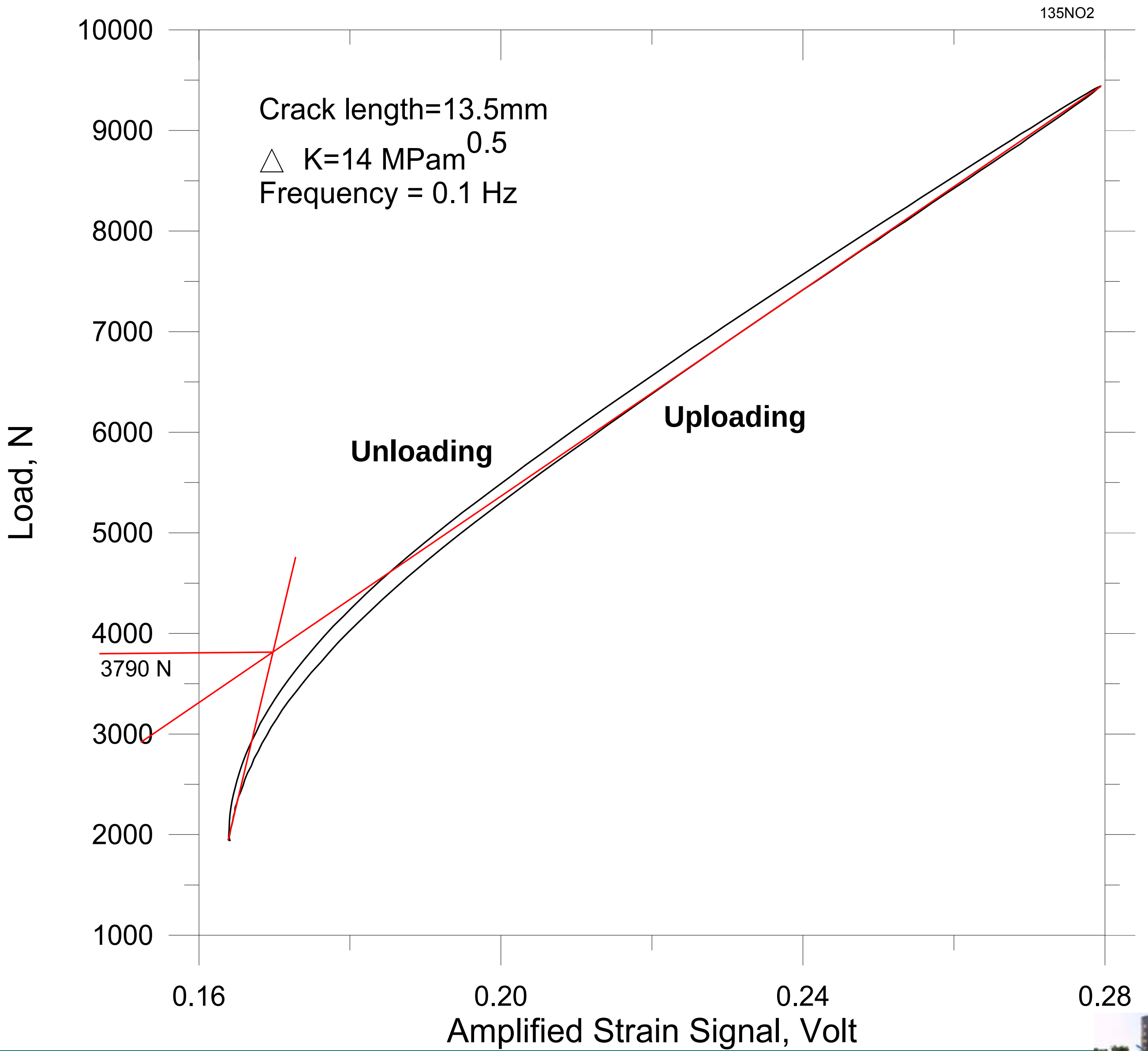

$$\Delta K_{eff} = \Delta K_{max} - \Delta K_{op}$$

The crack closure evolution along the crack length in the weld.

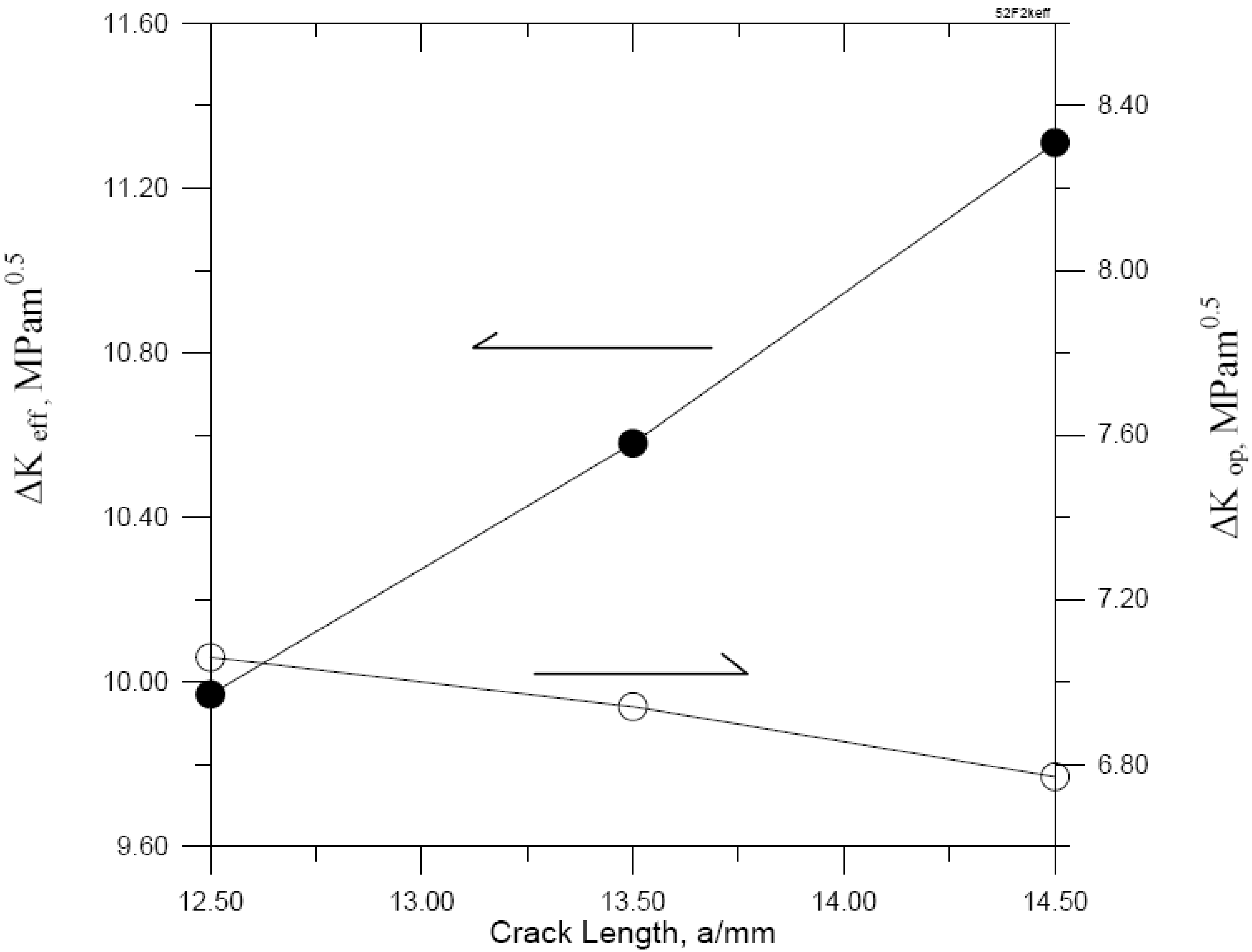

Macro-composition transition from the bottom to the center of the weld.

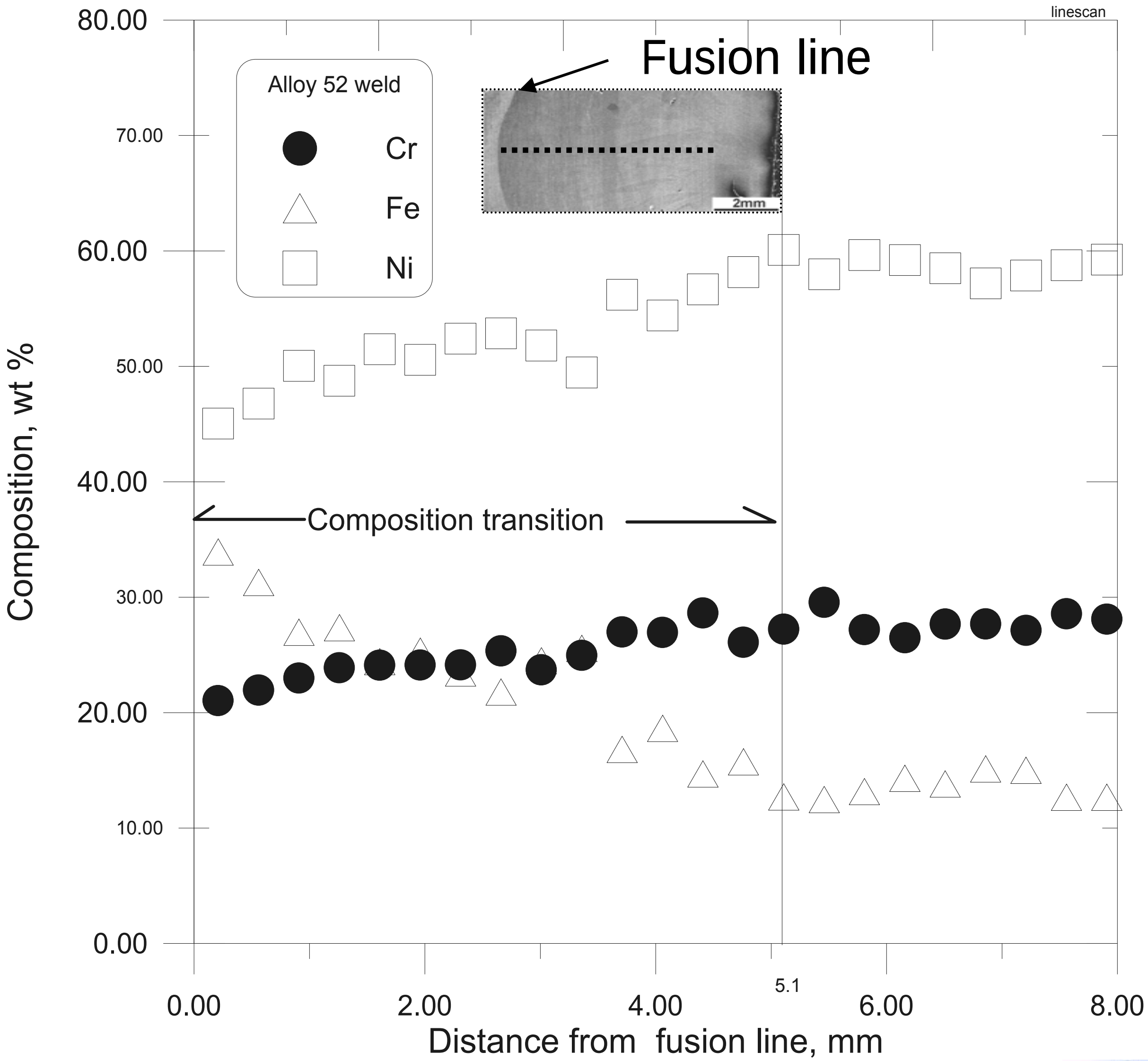

5. Conclusions

1) **Corrosion fatigue crack growth rates for the dissimilar metal weldments were observed to increase with crack advance under the nominal constant △K loading mode. This could be due to the effects of an increase in the tensile residual stress and a decrease in the crack closure in the Alloy 52 weld.**

2) **The tensile residual stress measured by a hole-drilling strain gauge method increased with the weld depth. The trend of stress distribution by numerical analysis agrees well with that for the experimental results.**

5. Conclusions

3) The crack closure effects in the weld were verified to decrease with the crack advance measured by the strain gauges ahead of the crack tip.

Thank you for your attention